Copper effect on cadmium sulfide thin films for spintronics: microstructures, morphological, photoluminescence and magnetic properties

M. Ahmed[a,*], A. Bakry[a], H. Dalir[b], E. R. Shaaban[c]
[a]Department of Physics, Faculty of Science, King Abdulaziz University, 80203 Jeddah21589, Saudi Arabia
[b]Department of Electrical and Computer Engineering, George Washington University, 20052, Washington, D.C., USA
[c]Physics Department: Faculty of Science, Al-Azhar University, P.O. 71452, Assiut, Egypt

$CdS_{1-x}Cu_x$ (with $0 \leq x \leq 0.10$) semiconductor thin films were successfully fabricated using electron beam evaporation. The effect of [Cu]/[S] on the structural properties of thin films was investigated using XRD, EDX, SEM and UV spectroscopy. Furthermore, the effects of different Cu concentrations on the optical parameters of these films are also reported. XRD analysis showed that the CdS1-xCux film was improved, showing a hexagonal polycrystalline structure with an increased Cu doping ratio. Furthermore, the size of the crystallites D decreases, while the microstrain ε-strain increases with increasing copper incorporation into the CdS lattice. The observed shift in the emission band of the photoluminescence spectrum confirms the substitution of Cu by the CdS lattice. Magnetization measurements using a vibrating sample magnetometer revealed hysteresis loops in Cu-doped CdS films and confirmed ferromagnetism at room temperature.

1. Introduction

I-VI semiconductors doped with transition metals such as Cu, Mn, Co, etc. are essential for their fundamental role in solar cell fabrication and advanced research materials and technological applications [1-3]. Among them, Cd-S is one of the very important semiconductors, offering energy gaps of 2.42 eV (cubic phase) and 2.57 eV (hexagonal phase) at room temperature. Furthermore, these semiconductor materials have interesting properties that enable them to be used in various recent optoelectronic applications such as nonlinear optics, visible light emitting diodes, lasers, and modern high-efficiency solar cells [4-6].

Doping Cd-S semiconducting materials with Copper (Cu) impurities could lead to large variation of the resistivity, band gap energy, photo electrical properties and also altering the type of semiconductor from "*n-type to p-type*" [7-9]. In fact , the presence of copper atoms in semiconducting are affected many interesting physico-chemical properties and reduce electrical resistance as Cd-S thin films have very high electrical resistance (10^7-10^8 Ω cm) [10, 11] .On the other hand, the optical properties of doped nano-materials vary from the corresponding host nano-materials as the dopants form deep trap levels serve as luminescence centers. Just a few reports have been reported on Cu^{2+} doped Cd-S nanoparticles [12, 13]. As mentioned above, the semiconducting materials doped with a small amount of metal impurities have unique properties that make them promising materials for potential applications, yet another purpose is to enhance the optical properties of Cd-S film doping with metal ions. Due to the lesser ionic radius of Cu^{2+} ions (0.73 A °) than the ionic radius of Cd^{2+} ions (0.97 A°), copper (Cu) was chosen as a doping source since Cu^{2+} ions can be easily incorporated into the Cd-S lattice. Thus, doping of Cd-S thin film with Cu^{2+} ions leads to new properties that differ significantly from undoped material. The

---

determination of Cu / Cd-S semi-conductor thin film materials (optical constants and optical band gap) is important not only for the discovery of the essential mechanism underlying these phenomenon but also for the exploitation and development of their prospective industrial application. The main objective in this work is to investigate the structural, morphological of $CdS_{1-x}Cu_x$ films prepared from evaporated electron beam gun. X-ray diffraction measurements have been carried out to detect the structural changes owing to doping of Cu of CdS films. The photoluminescence (PL) spectra of $CdS_{1-x}Cu_x$ the films have been carried out between the wavelengths ranging from 495 to 565 nm. Studies of the $CdS_{1-x}Cu_x$ magnetic properties have also been reported. The change in the deduced of (PL) spectra and magnetic properties can be interpreted in terms of micro-structural parameters.

2. Experimental procedures

$CdS_{1-x}Cu_x$ (x = 0, 0.02, 0.04, 0.06, 0.08, and 0.10 at. %) semiconductor materials was synthesized by a conventional solid-state reaction method, using ball milling technique. In the first step of the preparation, precursors of Copper (Cu 99.9% pure, particle diameter 422–2000 µm) and CdS powder with a purity of 99.999 % (M/S Sigma-Aldrich Co) were mixed in desired stoichiometric ratios in a ball mortar approximately 30 minutes. Mixed powders were then pressed into a disk-shaped pellet. Such pellets have been used as starting materials for the preparation of the thin film. Thin films of 1 µm of $CdS_{1-x}Cu_x$ were deposition electron beam evaporation method (Edward Auto 306) from a resistance heating quartz glass crucible onto glass substrates at a pressure of about 10^{-6} Pa.. The structure and the phases of $CdS_{1-x}Cu_x$ films were investigated by X-ray diffraction pattern (XRD Philips 1710). In addition, the configurational characteristics and elemental analysis of Cd, S and Cu are determined by the energy dispersion of the X-ray (EDAX) interfaced with a scanning electron microscope, SEM (JEOL JSM-6360LA, Japan) operating an accelerating voltage of 30 kV. The virtual error of the indicated elements unexceed 2%. The photoluminescence (PL) spectra of $CdS_{1-x}Cu_x$ the films have been carried out between the wavelength ranging from 495 to 565 nm using a spectrofluorometer (JASCO FP-6300) at RT. The excitation source is a Xenon lamp with a wavelength of 350 nm and a power of 150W. Using the vibrating sample magnetometer model (VSM-9600M-1, USA), studied the magnetic properties of the prepared films. The measurements were conducted in a maximum applied field of 7 kOe at temperature equal to RT.

3. Results and discussion

3.1. Structural analysis

The l EDX spectra of $CdS_{0.96}Cu_{0.04}$ and $Cd S_{0.9}Cu_{0.10}$ thin films respectively, shown in Fig. 1 (a and b). The appearance peaks indicate the stoichiometry of the composition Cd, S and Cu.
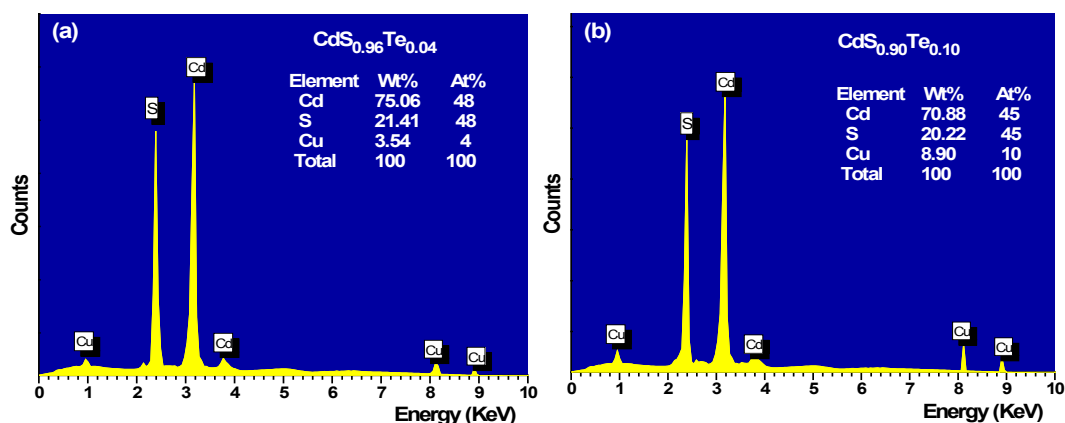

Fig. 1. EDAX spectra of CdS doped with Cu thin film (a) $CdS_{0.96} Cu_{0.04}$ (b) $Cd S_{0.9}Cu_{0.10}$

An increasing of Cu concentrations in the $CdS_{1-x}Cu_x$ films indicate that the Cu^{2+} ions has successfully acceptor incorporation into the Cd-S lattice. These results are in good conformity with the experimental composition utilized in the current system.

On the other hand, the X-ray diffraction (XRD) patterns can provide an efficient tool for determining the crystal structure of the Cu doped CdS. Fig. 2 (a, b) illustrates the structure of for $CdS_{1-x}Cu_x$ for both powder and films. it is clearly noticed from Fig. 2 (b) Cu doped Cd-S thin films exhibits three diffraction peaks matching to the diffraction angles 24.8, 26.5 and 28.3 appropriate to ("100", "002" and "101") planes of hexagonal phase, the standard diffraction planes shown in the films are matched to hexagonal structure of the [JCPDS card no. 00-001-0783], that is well agreement with the reported data on Cd-S system [14, 15].
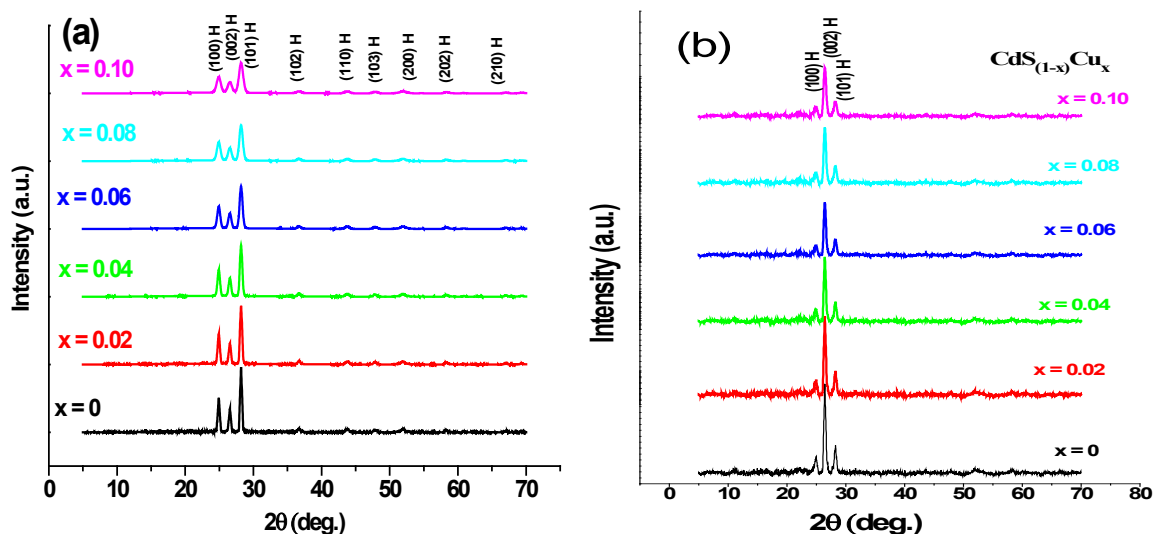

Fig. 2. XRD patterns of Cu doped CdS for (a) powder and (b) thin films.

The lattice constant of hexagonal crystals has two parameters (a and c) which can be calculate according to the formula [16, 17]

$$\frac{1}{d_{hkl}^2} = \frac{4}{3}\frac{h^2 + hk + k^2}{a^2} + \frac{l^2}{c^2} \tag{1}$$

where d_{hkl} is the inter-planer spacing and (h, k, l) are Miller indices for thin films these lattice constants can be obtained by Bragg's law $\lambda = 2d_{hkl}\sin\theta$ θ is the Bragg's diffraction angle of the peak [13]. More than the lattice constants 'a', 'c' for CdS1-xCux films can be determined form XRD data using $a = b = \lambda\left(\sqrt{3}\sin\theta\right)^{-1}$ and $c = \lambda\left(\sin\theta\right)^{-1}$ respectively,. it is interesting notice that the lattice parameter decreases with an increase Cu concentration demonstrated in Fig. 3. These results may be attributed to the different atomic radii of Cu ions and their positions in Cd-S lattice, that implies a decline in the volume of the unit cell [6, 14].
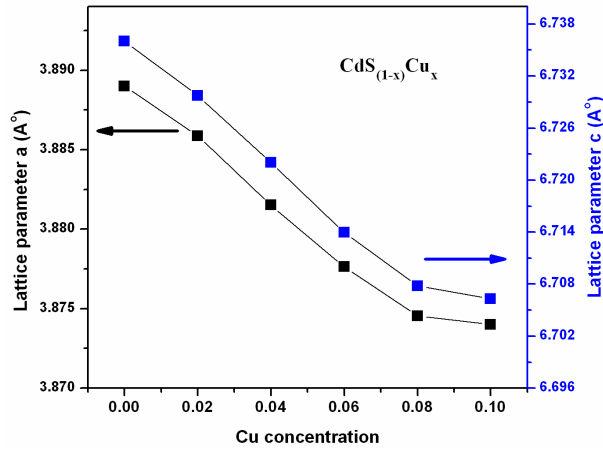
Fig. 3. Lattice parameters "a" and "c" of Hexagonal polycrystalline as a function of CdS doped with Cu thin films.

In addition, to evaluation of the X-ray diffraction data. The average crystal size "D" for $CdS_{1-x}Cu_x$ thin films can be obtained utilizing Debye Scherrer's formula[18]

$$D = \frac{0.89\lambda}{\beta \cos(\theta)} \tag{2}$$

where β is the full width at half maximum (FWHM) and λ is the wavelength. The lattice micro-strain (ε) can be estimated from the following equation [19]

$$\text{Micro - strain } \varepsilon = \frac{\beta}{4\tan(\theta)} \tag{3}$$

The obtained values of crystallite size D and the lattice micro-strain ε are illustrate in fig. 4. It is clearly seen that the crystallite size D is reduced whereas the micro-strain ε strain increase with enhancement the copper incorporation in Cd-S lattice. The reason for this may be that the substitution of Cu^{2+} ions disturbs the Cd–S lattice and decrease the nucleation and subsequent growth rate[6, 17]. This change leads to lattice contraction, an increase in the micro- strain and a decrease in in crystallite size[20].
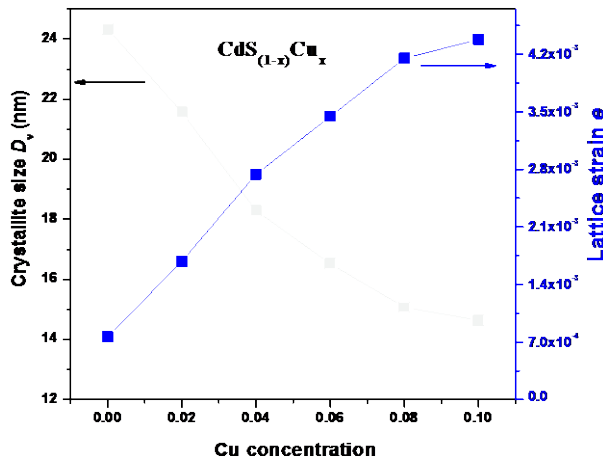

Fig. 4. Cu doping concentrations dependence of the crystallite size D and strain ε formed in CdS thin films.

The thin films of the CdS, $CdS_{0.96}Cu_{0.04}$ and $CdS_{0.90}Cu_{0.10}$ scanning electron microscope images (SEM) are shown in Fig. 5 (a, b and c). The film CdS was found to be less dense than the films CdS:Cu. The denser CdS:Cu films are, however, obtained with increased concentration of Cu dopants. The value of average grain sizes is clearly greater than the calculated crystallite sizes of XRD studies because the grains consist of many crystallites [21].
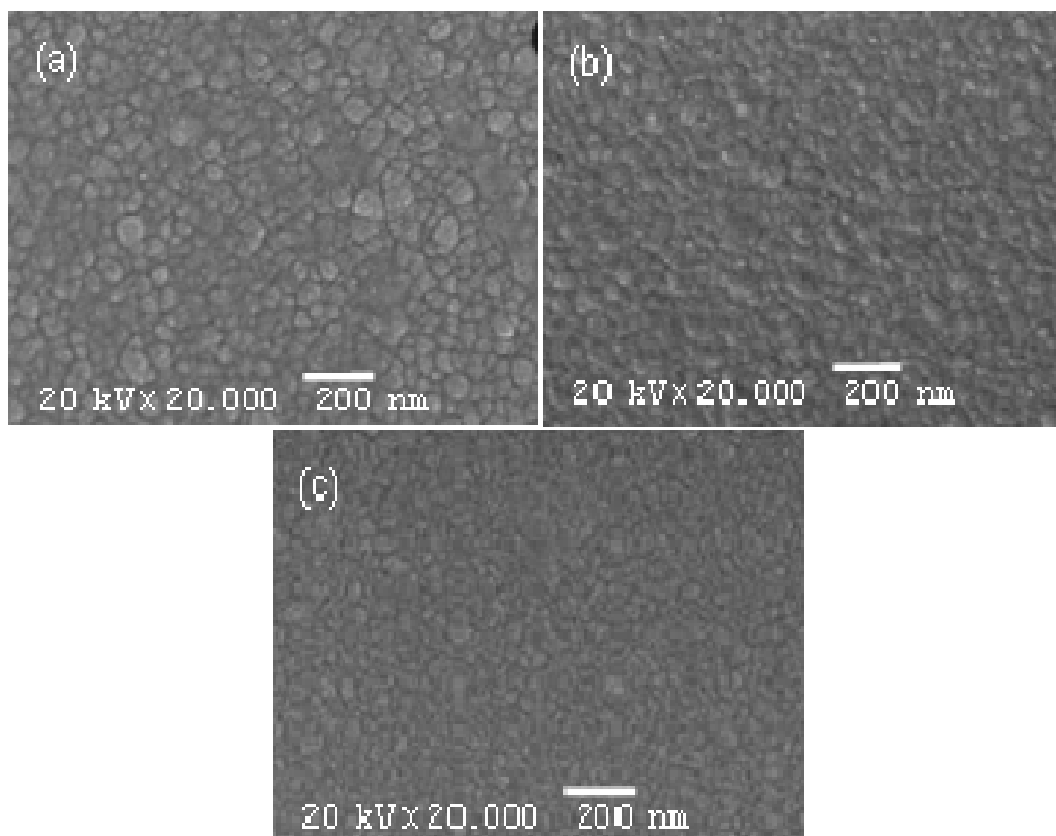

Fig. 5. Scanning electron microscope images (SEM) of (a) CdS, (b) $CdS_{0.96}Cu_{0.04}$,
(c) $CdS_{0.90}Cu_{0.10}$ thin films.

3.2. Photoluminescence (PL) spectra

Figure 6 shows the PL spectra of CdS1-xCux films at room temperature. The excitation energy is 3.5 eV (350 nm). After adding Cu2+, the PL intensity of the CdS films decreased. The decrease in PL intensity of samples with higher Cu2+ doping levels can be attributed to the increase in surface defects, leading to an increase in nonradiative transitions. In the extended wavelength range from 495 to 565 nm, two bands are clearly visible. The wavelengths of these two bands are about 510 and 530 nm, which is longer than the wavelength of the bandgap energy, which is about 505 nm. Since the wavelength of the first peak is higher than that of the second peak, the first peak and the second peak can be assigned according to the shallowness and depth of the trap. Since the displacement of the deep traps is negligible, transitions from the deep trap reference should not change their energies by decreasing with increasing particle size. But as the particle size decreases, the shallow well moves with the intrinsic band. Therefore, the position of the second band is fixed and the initial band should move to lower energies with decreasing particle size [22]. The luminescence mechanism of Cu-doped CdS thin films can be analyzed as follows: when CdS absorbs photons, electrons are excited and trapped by vacancies from the valence band to the conduction band. The recombination of copper defects and excited states changes the surface trap states, which improves transitions and broadens the luminescence range [23].
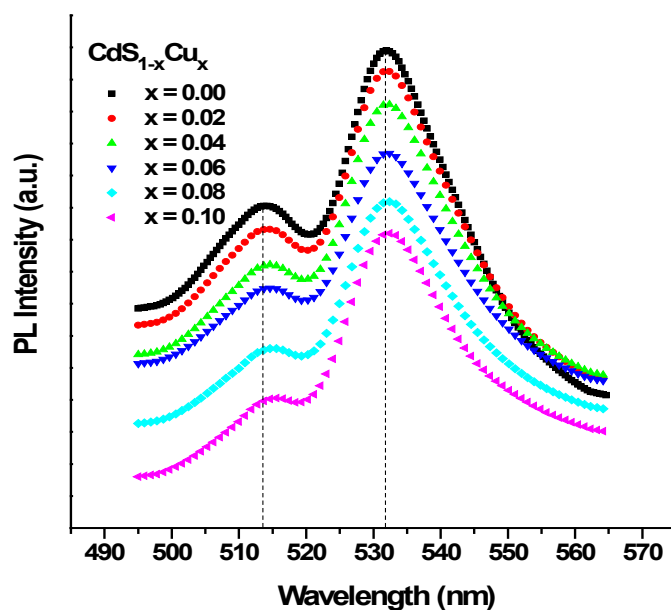
Fig. 6. Photoluminescence spectra for for CdS$_{1-x}$Cu$_x$ thin films.

3.3. Magnetic properties

By applying parallel magnetic fields to the film planes at RT, the magnetic characteristics of thin films of CdS(1-x)Cux were examined. Fig. 7 shows the hysteresis M-H plots for the magnetization measurements M(H) against the magnetic field for the CdS(1-x)Cux thin films. All of the results were collected after the diamagnetic contribution from the glass substrates was removed. The magnetization plot of pure CdS exhibits a diamagnetic-like behaviour with a negative magnetic susceptibility [24], as would be predicted given its inherent diamagnetic nature. Figure 7 shows the M-H curves for doped CdS(1-x)Cux films at 283 K. The magnetism in doped CdS: Cu films may be the result of interactions, as this figure demonstrates a hysteretic trend and reveals a ferromagnetic characteristic with a tiny coercive field and low remanence of soft ferromagnetism. The source of ferromagnetism in Cu doped CdS, a diluted magnetic semiconductor (DMS) with a modest fraction of up to 10%, is still a contentious issue that is not entirely clear. However, two precise mechanisms resulting from a number of theories are frequently expected to explain the ferromagnetism of DMSs: the carrier-induced Ruderman-Kittel-Kasuya-Yosida substitute interaction (RKKY interaction) or bound magnetic polarons (BMPs) producing long-range magnetic order [25, 26]. The purpose of the current work is to investigate the mechanism by which the carrier causes ferromagnetism (dual exchange mechanism) in Cu-doped CdS films. It is possible that the substitution of Cu ions for Cd ions is what caused the ferromagnetic behaviour observed in the CdS lattice. Similar ferromagnetic results were found by Singh [27] and Kumar [28].
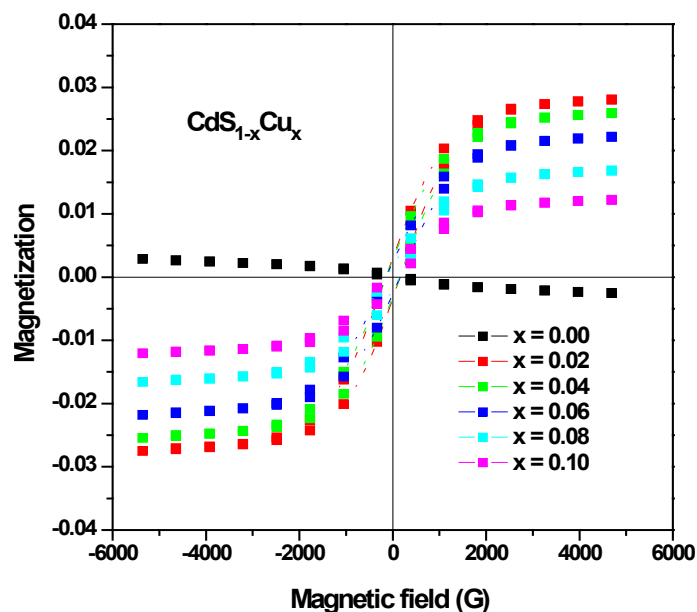
Fig. 7. M-H loop CdS$_{1-x}$Cu$_x$ thin films at RT.

4. Conclusions

The electron beam evaporation approach was successfully used to create composite CdS that was both pure and doped with Cu. According to XRD data, the examined thin films have a (002) plane as their preferred crystal growth orientation, and they have a hexagonal polycrystalline structure. As the Cu doping ratio increased, the crystallite size and micro-strain and strain increased. In CdS(1-x)Cux films, the PL intensity rises with increasing Cu concentration, and the observed shift of the photoluminescence spectrum's first peak from 510 nm (near the energy gap) to a higher wavelength supported the substitution of Cu into the Cd-S lattice. Magnetic tests at T = 283 K revealed ferromagnetism in all Cu-doped CdS sheets. It is possible to attribute the ferromagnetic behaviour seen in the CdS lattice to the substitution of Cu ions by Cd ions.

References

[1] Y. Gu, E.-S. Kwak, J. Lensch, J. Allen, T.W. Odom, L.J. Lauhon, Applied Physics Letters, 87 (2005) 043111; https://doi.org/10.1063/1.1996851
[2] Emam-Ismai M l, El-Hagary M, Shaaban E.R., Althoyaib S, Journal of alloys and compounds 2012, 529, 113-121; https://doi.org/10.1016/j.jallcom.2012.03.027
[3] Shaaban E,R,, A Almohammedi, Ali G.A.M., Chong K.F., A Adel, A Ashour, Optik 2018, 164, 527-537; https://doi.org/10.1016/j.ijleo.2018.03.001
[5] A.A. Ziabari, F. Ghodsi, Growth, Solar energy materials and solar cells, 105 (2012) 249-262; https://doi.org/10.1016/j.solmat.2012.05.014
[6] A. Pan, H. Yang, R. Yu, B. Zou, Nanotechnology, 17 (2006) 1083-1086; https://doi.org/10.1088/0957-4484/17/4/040
[7] V. Singh, P.K. Sharma, P. Chauhan, Materials Characterization, 62 (2011) 43-52;

https://doi.org/10.1016/j.matchar.2010.10.009

[8] El-Naim A, Solieman A., Shaaban E. R., Materials in Electronics 31 (4) (2020) 3613-3621; https://doi.org/10.1007/s10854-020-02916-8

[9] Alzaid M.,. Mohamed W. S, El-Hagary M., Shaaban E. R., Hadia N. M. A., Optical Materials 2021, 118, 111228; https://doi.org/10.1016/j.optmat.2021.111228

[10] Y. Kashiwaba, K. Isojima, K. Ohta, Solar Energy Materials and Solar Cells, 75 (2003) 253-259; https://doi.org/10.1016/S0927-0248(02)00167-8

[11] M. Muthusamy, S. Muthukumaran, Optik, 126 (2015) 5200-5206; https://doi.org/10.1016/j.ijleo.2015.09.186

[12] S. Muthukumaran, R. Gopalakrishnan, Optical Materials, 34 (2012) 1946-1953; https://doi.org/10.1016/j.optmat.2012.06.004

[13] F. Atay, S. Kose, V. Bilgin, I. Akyuz, Materials Letters, 57 (2003) 3461-3472; https://doi.org/10.1016/S0167-577X(03)00100-9

[14] H. Kato, J. Sato, T. Abe, Y. Kashiwaba, Photoluminescence of p-type CdS:Cu thin films, physica status solidi (c), 1 (2004) 653-656; https://doi.org/10.1002/pssc.200304152

[15] C. Unni, D. Philip, K.G. Gopchandran, Spectrochimica Acta Part A: Molecular and Biomolecular Spectroscopy, 71 (2008) 1402-1407; https://doi.org/10.1016/j.saa.2008.04.023

[16] Ylrich, Zachariaben., Z. Kristallogr, Dana's System of Mineralogy, 7th Ed. , (62, 262, (1925).

[17] G. Krishnaiah, N.M. Rao, D.R. Reddy, B. Reddy, P.S. Reddy, Journal of crystal growth, 310 (2008) 26-30; https://doi.org/10.1016/j.jcrysgro.2007.10.013

[18] B.D. Cullity, Elements of X-ray Diffraction, Addison-Wesley Publishing, 1956.

[19] M. Shaban, M. Mustafa, A.M. El Sayed, Materials Science in Semiconductor Processing, 56 (2016) 329-343; https://doi.org/10.1016/j.mssp.2016.09.006

[20] S. Muthu Kumaran, R. Gopalakrishnan, Journal of Sol-Gel Science and Technology, 62 (2012) 193-200; https://doi.org/10.1007/s10971-012-2708-8

[21] Shaaban ER, Kansal I, Mohamed S., Ferreira J MF. s. Physica B: Condensed Matter. 2009; 404(20):3571-3576; https://doi.org/10.1016/j.physb.2009.06.002

[22]. K.K. Nanda, S.N. Sahu, Solid State Commun. 111, 671 (1999); https://doi.org/10.1016/S0038-1098(99)00268-9

[23] C. Unni, D. Philip, K.G. Gopchandran, Spectrochim. Acta A 71, 1402 (2008); https://doi.org/10.1016/j.saa.2008.04.023

[24] Tahashi M, Wu Z, Goto H, Hayashi Y, Ido T. Mater Trans. 2009;50(4):719-22; https://doi.org/10.2320/matertrans.MBW200812

[25] N. H. Hong, J. Sakai, N. T. Huong, Poirot N, Ruyter. Phys Rev B. 72(4): (2005) 045336; https://doi.org/10.1103/PhysRevB.72.045336

[26] J. Coey, M. Venkatesan, C. Fitzgerald. Nat Mater. 4(2): (2005)173; https://doi.org/10.1038/nmat1310

[27]. J. Singh, N. Verma.. J Supercond Novel Magn. 27(10) (2014), 2371-7; https://doi.org/10.1007/s10948-014-2603-3

[28] T. R. Kumar, P. Prabukanthan, G. Harichandran, J. Theerthagiri, S. Chandrasekaran, J. Madhavan.. Ionics. 23(9), (2017) 2497-507; https://doi.org/10.1007/s11581-017-2090-1